UNIAXIAL ELASTIC-PLASTIC WAVE PROPAGATION

by H. OCKENDON, J. R. OCKENDON, P. D. HOWELL,

(*Mathematical Institute, University of Oxford, Andrew Wiles Building, Woodstock Road, Oxford, OX2 6GG, UK*)

and S. J. THOMSON[‡]

(*Department of Mathematics, Massachusetts Institute of Technology, Cambridge, Massachusetts 02139, USA*)

[To be inserted by the editor]

Summary

This paper considers the uniaxial elastic-plastic response of a solid slab subject to a velocity applied to one boundary, over time scales on which both elastic and plastic waves can propagate. We briefly describe a simple model in which the amplitudes are small enough for these waves to satisfy linear wave equations, although the full problem is still nonlinear because of the presence of an unknown free boundary separating elastic and plastic regions. Examples are given which show that the presence of residual stress can cause the pattern of elastic and plastic regions in the (X, t)-plane to be surprisingly complicated.

1. Introduction

We consider a simple model for the uniaxial elastic-plastic deformation of a metal sample. We will only consider amplitudes that are so small that, in regions where the yield stress has not been attained, the field equation is the scalar linear wave equation for p-waves in an elastic solid. Moreover, with the assumption that any plastic deformation is incompressible, the field equation in regions where there is plastic flow is a similar wave equation but with a slower wave speed. Within each of these regions, singularities may propagate along characteristics. However, we will see that the elastic-plastic interface may involve regions of space-time where the yield stress is attained but there is no plastic flow. Also, when the metal is sequentially loaded and unloaded, we show that this interface may move faster than the elastic wave speed as the residual stress builds up.

The analysis herein is built on the more detailed general theory described in (**8**, **9**), which in turn relies on earlier works (**2**, **3**), and references therein. Pioneering research in this area was done by (**4**, **5**) whose approach differs from ours in that the effect of residual stress is modelled by applying a prescribed spatially varying yield stress; also these papers only consider waves in material that is unbounded in either direction. The extra complications that can arise when the amplitudes are large enough for shock waves to occur are described in (**1**).

We organise the paper as follows. In §2 we begin with a brief derivation of our model, consisting of two linear wave equations that apply in elastic and plastic regions respectively,

[‡] Corresponding author: thomsons@mit.edu

along with coupling conditions that apply at interfaces where the material switches from elastic to plastic or *vice versa*. In §3 we analyse the possible local configurations allowed by the model in which elastic and plastic regions in (x,t)-space are separated by a curve on which the stress and velocity have a slope discontinuity. In the remainder of the paper, the global effects of the propagation and interaction of such elastic-plastic free boundaries are illustrated by analysing in detail two specific examples. In §4 we investigate a material half-space subject to sequential loading and unloading tractions, and in §5 we study the wave reflections that occur in a finite slab of metal. Finally, we discuss our results and draw some conclusions in §6.

2. Mathematical model

2.1 *Uniaxial geometry and conservation laws*

Throughout, we will only consider material in the region $X > 0$ in a (Lagrangian) reference frame (X, Y, Z) under uniaxial displacement, so that the Eulerian position of an element is given by $\mathbf{x} = (x(X,t), 0, 0)$ after time t. We assume that the stress tensor $\boldsymbol{\tau}$ and strain tensor $\mathbf{e}$ also observe the uniaxial geometry, so that they take the forms

$$\boldsymbol{\tau} = \operatorname{diag}\big(\tau_1(X,t), \tau_2(X,t), \tau_2(X,t)\big), \qquad \mathbf{e} = \operatorname{diag}\big(e_1(X,t), e_2(X,t), e_2(X,t)\big). \tag{2.1}$$

The axial velocity and the strain components are then given by

$$u = \frac{\partial x}{\partial t}, \qquad e_1 = \frac{\partial x}{\partial X} - 1. \qquad e_2 = 0. \tag{2.2}$$

Conservation of mass and momentum in the assumed one-dimensional geometry leads to the governing equations

$$\frac{\partial e_1}{\partial t} - \frac{\partial u}{\partial X} = 0, \qquad \rho_0 \frac{\partial u}{\partial t} - \frac{\partial \tau_1}{\partial X} = 0, \tag{2.3}$$

where ρ_0 is the density in the reference state, assumed to be constant. To close the problem, we require a constitutive relation between the stress τ_1 and the strain e_1, which will depend on whether the material is deforming elastically or plastically.

2.2 *Strain decomposition*

To describe a material that may undergo both reversible elastic deformation and permanent plastic flow, we now decompose the strain into elastic and plastic components by writing

$$\mathbf{e} = \mathbf{e}^e + \mathbf{e}^p. \tag{2.4}$$

Such an additive decomposition is appropriate provided the strains are sufficiently small, in particular if they are small enough for linear elasticity to apply throughout. For strains of $O(1)$, a multiplicative decomposition of the deformation gradient is required instead, as described in (**3**, **9**).

We assume that the elastic and plastic strain tensors both have the uniaxial structure (2.2). For purely unidirectional displacement, the decomposed strain components must therefore satisfy

$$e_1^e + e_1^p = e_1, \qquad e_2^e + e_2^p = 0. \tag{2.5}$$

We also assume that the plastic deformation is incompressible[†], and hence

$$e_1^p + 2e_2^p = 0. \tag{2.6}$$

2.3 *Model closure*

2.3.1 Constitutive relations

As suggested above, we assume a linear elastic relation between the stress and the elastic strain components, i.e.

$$\tau_1 = (\lambda + 2\mu)e_1^e + 2\lambda e_2^e, \tag{2.7}$$

$$\tau_2 = \lambda e_1^e + 2(\lambda + \mu)e_2^e, \tag{2.8}$$

where λ and μ are the Lamé constants.

For the plastic deformation, we adopt a perfect plasticity model with a constant yield stress τ_Y, thereby neglecting effects such as hardening and rate dependence. We assume that plastic flow commences once the shear stress reaches the yield stress τ_Y, but that the shear stress can never then exceed this critical value. In uniaxial strain, the maximal shear stress is measured by the quantity $|\tau_1 - \tau_2|$ and the material remains elastic whenever

$$|\tau_1 - \tau_2| < \tau_Y. \tag{2.9a}$$

When considering deformations in which pristine material is first plasticised and then returned to an elastic state, the material may retain a residual strain and corresponding residual stress. Hence, in the elastic regime, the plastic deformation e_1^p need not be zero although it must remain constant in time so that, as long as (2.9a) holds, we have

$$\frac{\partial e_1^p}{\partial t} = 0. \tag{2.9b}$$

When the shear stress reaches the yield stress, plastic flow may commence in which

$$|\tau_1 - \tau_2| = \tau_Y. \tag{2.10a}$$

In addition the resulting energy dissipation must be non-negative which means that

$$(\tau_1 - \tau_2)\frac{\partial e_1^p}{\partial t} \geqslant 0. \tag{2.10b}$$

The two possibilities (2.9) and (2.10) may be handily combined into the complementarity conditions

$$\big(|\tau_1 - \tau_2| - \tau_Y\big)\frac{\partial e_1^p}{\partial t} = 0, \qquad |\tau_1 - \tau_2| \leqslant \tau_Y, \qquad (\tau_1 - \tau_2)\frac{\partial e_1^p}{\partial t} \geqslant 0. \tag{2.11}$$

In principle, (2.3), (2.5), (2.6), (2.7), (2.8) and (2.11) form a system of 8 equations for the 8 unknowns u, τ_1, τ_2, e_1, e_1^e, e_1^p, e_2^e and e_2^p. To facilitate the subsequent discussion, we will henceforth work with the axial velocity $u = \partial e_1/\partial t$ and the axial stress τ_1 as our dependent variables, with the plastic strain e_1^p and the shear stress $\sigma = \tau_1 - \tau_2$ as auxiliary variables.

[†] as shown in (**2**), the assumption of incompressibility is equivalent to the use of an associated flow rule

2.3.2 The elastic state

In the elastic state we can use (2.5), (2.6) and (2.7) to write

$$\tau_1 = (\lambda + 2\mu)e_1 - 2\mu e_1^p \tag{2.12}$$

which leads from (2.3) and (2.9a) to

$$\frac{\partial \tau_1}{\partial t} - (\lambda + 2\mu)\frac{\partial u}{\partial X} = 0, \qquad \rho_0 \frac{\partial u}{\partial t} - \frac{\partial \tau_1}{\partial X} = 0. \tag{2.13}$$

Thus we see that u and τ_1 satisfy linear wave equations with the elastic p-wave speed $c_e = \sqrt{(\lambda + 2\mu)/\rho_0}$.

In view of (2.12), we now define the *residual stress* τ_R in an elastic region by

$$\tau_R(X) = -2\mu e_1^p; \tag{2.14}$$

this is the time-independent axial stress that is the difference between the actual stress and that which would have occurred in the purely elastic deformation of a pristine material.

2.3.3 The plastic state

When the material is deforming plastically we use (2.5)–(2.8) with (2.10a) to find that

$$\tau_1 = \left(\lambda + \frac{2}{3}\,\mu\right) e_1 + \frac{2}{3}\,(\tau_1 - \tau_2), \tag{2.15}$$

and then (2.3) becomes

$$\frac{\partial \tau_1}{\partial t} - \left(\lambda + \frac{2}{3}\mu\right)\frac{\partial u}{\partial X} = 0, \qquad \rho_0 \frac{\partial u}{\partial t} - \frac{\partial \tau_1}{\partial X} = 0. \tag{2.16}$$

Thus the plastic flow is also modelled by a linear wave equation but now with plastic wave speed $c_p = \sqrt{K/\rho_0}$, where $K = \lambda + 2\mu/3$ is the elastic bulk modulus; such waves were observed as long ago as 1948 by (**6**). The plastic wave speed c_p is always less than the elastic wave speed c_e.

2.4 *Dimensionless model*

We non-dimensionalise using a reference length-scale L and velocity scale U as follows:

$$x = L\tilde{x}, \qquad t = \frac{L}{c_p}\,\tilde{t}, \qquad u = U\tilde{u}, \qquad (\tau_1, \tau_R, \tau_Y, \sigma) = \rho_0 c_p U\,(\tilde{\tau}_1, \tilde{\tau}_R, \tilde{\tau}_Y, \tilde{\sigma})\,. \tag{2.17}$$

Then, in non-dimensional terms, the plastic wave speed is unity and the elastic wave speed

$$c = \frac{c_e}{c_p} = \sqrt{\frac{\lambda + 2\mu}{\lambda + \frac{2}{3}\mu}} > 1. \tag{2.18}$$

With the tildes dropped henceforth, the dimensionless model is as follows.

When the material is elastic, the dimensionless versions of the wave equations (2.13) take the forms

$$\frac{\partial \tau_1}{\partial t} - c^2 \frac{\partial u}{\partial X} = 0, \tag{2.19a}$$

$$\frac{\partial u}{\partial t} - \frac{\partial \tau_1}{\partial X} = 0. \tag{2.19b}$$

From (2.14) we obtain an auxiliary equation for the dimensionless shear stress

$$\sigma = \frac{3}{2c^2}\left((c^2-1)\tau_1 + \tau_R(X)\right), \tag{2.19c}$$

and the material remains elastic while the yield condition

$$|\sigma| \leqslant \tau_Y \tag{2.19d}$$

is satisfied.

When the material is plastic, we instead obtain the dimensionless system of equations

$$\frac{\partial \tau_1}{\partial t} - \frac{\partial u}{\partial X} = 0, \tag{2.20a}$$

$$\frac{\partial u}{\partial t} - \frac{\partial \tau_1}{\partial X} = 0, \tag{2.20b}$$

$$\sigma = \pm \tau_Y. \tag{2.20c}$$

Here and henceforth the $\pm$ symbol denotes that the material is under tension or compression respectively. The material remains plastic as long as the plastic strain rate satisfies the dissipation condition in (2.10b), which, from (2.15), is equivalent to the inequality

$$\pm \frac{\partial \tau_1}{\partial t} \geqslant 0. \tag{2.20d}$$

2.5 *Elastic–plastic solutions*

We note that there is a class of solutions that simultaneously satisfy *both* the elastic model (2.19) *and* the plastic model (2.20), namely

$$\tau_1 = a_1 X + a_2, \qquad u = a_1 t + a_3, \tag{2.21a}$$

$$\tau_R = -\left(c^2-1\right)(a_1 X + a_2) \pm \frac{2}{3} c^2 \tau_Y, \qquad \sigma = \pm \tau_Y, \tag{2.21b}$$

where a_1, a_2, a_3 are constants. Such a solution describes regions where elastic material has reached the yield stress but has not yet commenced plastic flow, or alternatively plastic material that is just about to return to being elastic.

3. Solutions with discontinuities

3.1 *Problem definition and general observations*

Having established the equations governing both elastic and plastic deformations, we now examine the conditions to be imposed at an internal acceleration wave across which the

dependent variables are all continuous but their first derivatives are not. Jumps in the first derivatives of τ_1 and u can propagate along the respective characteristics within both the elastic and plastic regions. However, the situation is not so clear when we have a moving boundary separating elastic from plastic material. Without loss of generality, let us consider such a boundary moving in the positive X-direction with propagation speed $V > 0$. We denote the limiting values of the dependent variables on either side of the moving discontinuity using E and P superscripts in the elastic and plastic regions respectively. Below we will analyse separately the cases where the material is elastic ahead of and plastic behind the moving boundary, and *vice versa*.

3.2 *Elastic to plastic transitions*

In the first instance, suppose the material is elastic ahead of the boundary and plastic behind it so that initially elastic material yields and becomes plastic as it crosses the boundary. By continuity of the shear stress, we must have

$$\left(\frac{\partial}{\partial t} + V\frac{\partial}{\partial X}\right)\sigma = 0 \tag{3.1}$$

on both sides of the boundary. On the elastic side, for the yield condition (2.19d) to be satisfied just ahead of the boundary, we must have

$$\pm\frac{\partial \sigma^E}{\partial X} \leqslant 0 \tag{3.2}$$

and hence

$$\pm\frac{\partial \tau_1^E}{\partial t} \geqslant 0, \tag{3.3}$$

when we use (2.19c) to evaluate σ on the elastic side. Comparing with (2.20d), we see that $\partial\tau_1/\partial t$ has the same sign on both sides of the elastic-plastic boundary.

Now let us examine the information that we have to determine the first derivatives of the dependent variables on either side of the boundary. Continuity of τ_1 and u implies the relations

$$\left[\frac{\partial \tau_1}{\partial t} + V\frac{\partial \tau_1}{\partial X}\right]_P^E = 0, \qquad \left[\frac{\partial u}{\partial t} + V\frac{\partial u}{\partial X}\right]_P^E = 0. \tag{3.4}$$

We also know that τ_1^E and u^E satisfy (2.19a) and (2.19b), and similarly τ_1^P and u^P satisfy (2.20a) and (2.20b). In total, then, we have six equations for eight unknowns, namely the X- and t-derivatives of τ_1^E, τ_1^P and u^E, u^P. By eliminating between these equations, we obtain

$$\left(1 - \frac{V^2}{c^2}\right)\frac{\partial \tau_1^E}{\partial t} = \left(1 - V^2\right)\frac{\partial \tau_1^P}{\partial t}. \tag{3.5}$$

Since, as argued above, the two time derivatives of τ_1 must have the same sign, we conclude that either $V \in (0, 1)$ or $V \in (c, \infty)$, for an elastic-plastic boundary propagating into an elastic region.

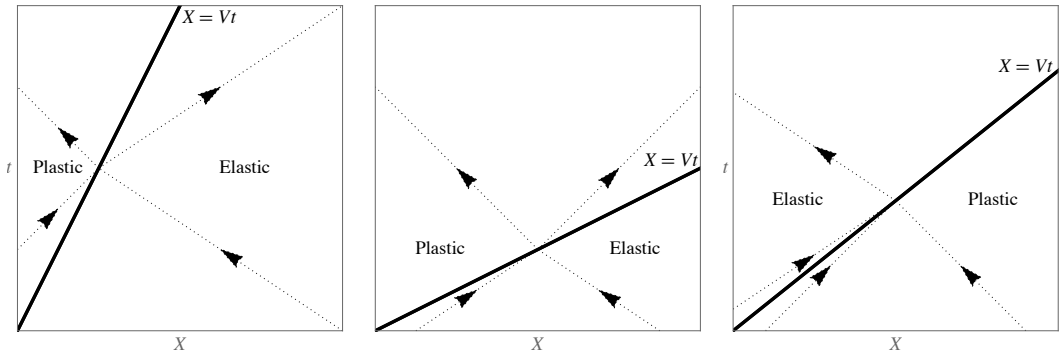

(a) $V < 1$ (b) $V > c$ (c) $1 < V < c$

Fig. 1 Schematics showing three possible scenarios where an elastic-plastic slope discontinuity propagates at speed V. The characteristics are plotted using dotted arrows. In cases (a) and (b), the discontinuity propagates into an elastic region, with either $V < 1$ or $V > c$; in case (c), the discontinuity propagates into a plastic region, with $V \in (1, c)$.

Alternatively a simple causality argument may be used to reach the same conclusion. Since the yield condition $\sigma^E = \pm\tau_Y$ holds on the boundary, we need two further pieces of information to determine the values of τ_1 and u on the boundary as well as the boundary speed V. There are only two possible scenarios in which two sets of characteristics propagate into the boundary as time increases. If $V < 1$, then both the plastic characteristics with $\dot{X} = +1$ and the elastic characteristics with $\dot{X} = -c$ enter the boundary . Alternatively, if $V > c$, then the elastic characteristics $\dot{X} = \pm c$ both enter the boundary, and both characteristics exit on the plastic side. Thus the elastic-plastic free boundary can be causal only if V lies in one of the two ranges identified above. The patterns of characteristics entering and exiting the boundary in either case are shown schematically in Figure 1(a) and (b) respectively. Note that in the second case, we have the somewhat surprising result that the free boundary travels faster than the elastic wave-speed.

3.3 *Plastic to elastic transitions*

Analogous arguments work for the case of an elastic-plastic boundary propagating into a plastic region at speed $V > 0$. By exploiting the continuity and the equations satisfied by τ_1 and u on either side of the boundary, as above, we again obtain equation (3.5). This time, however, for the yield condition (2.19d) to be satisfied in the elastic region just behind the moving boundary, we now require

$$\pm\frac{\partial \tau_1^E}{\partial t} \leqslant 0, \tag{3.6}$$

so that $\partial\tau_1/\partial t$ must change sign across the boundary. We deduce from (3.5) that an elastic-plastic boundary propagates into a plastic region at a speed V that lies between the two wave-speeds 1 and c. As above, the same conclusion may be reached by imposing the causality condition; now three sets of characteristics must enter the boundary since the yield condition is always satisfied in the plastic region. Thus there must be two sets of

incoming plastic characteristics and one set of incoming elastic characteristics, as shown schematically in Figure 1(c).

In the next section, we will demonstrate the complicated interactions between elastic and plastic boundaries that can occur by focusing on the concrete problem of a half-space, one face of which is subject to a specified loading and unloading.

4. Compression and tension of a half-space

4.1 *Compression*

We consider the solution of the problem (2.19)–(2.20d) for a half-space $X > 0$ containing material that is initially stationary and unstressed, i.e. subject to the initial conditions

$$u = \tau_1 = \tau_R = 0 \quad \text{when } t = 0,\ X > 0. \tag{4.1}$$

Now suppose that a linearly increasing velocity is imposed at the face $X = 0$ such that

$$u = t \quad \text{when } t > 0,\ X = 0. \tag{4.2}$$

The solution of the resulting problem is simplified since the dependent variables are everywhere piecewise linear functions of X and t.

The initially unstressed material is in the elastic state, so we start by solving the elastic system (2.19). The material remains undisturbed in $X > ct$ ahead of the leading elastic characteristic, behind which there is a compressive elastic wave with

$$\tau_1 = X - ct, \qquad u = t - \frac{X}{c}, \qquad \tau_R = 0, \qquad \sigma = \frac{3\left(c^2-1\right)}{2c^2}\,(X - ct). \tag{4.3}$$

The solution (4.3) fails when the yield condition (2.19d) is violated, which occurs when

$$t = \frac{2c\tau_Y}{3\left(c^2-1\right)} + \frac{X}{c} = t_* + \frac{X}{c}, \tag{4.4}$$

say, and we conclude that (4.3) holds in the range $0 < X/c < t < t_* + X/c$, marked as E_1 in Figure 2.

Thereafter, the material yields, and we switch to the plastic system of equations (2.20), obtaining the solution

$$\tau_1 = X - t - (c-1)t_*, \qquad u = t - X, \qquad \sigma = -\tau_Y. \tag{4.5}$$

However, the plastic solution (4.5) is valid in the region, marked P_1 in Figure 2, behind the leading plastic characteristic, i.e. in $0 < X < t - t_*$. There is therefore a region, labelled C_1 in Figure 2, between the trailing elastic characteristic and the leading plastic characteristic, in which neither solution (4.3) nor (4.5) holds. We find that the solution in this intermediate region $X/c < t - t_* < X$ is constant, with

$$\tau_1 = -\frac{2c^2\tau_Y}{3\left(c^2-1\right)}, \qquad u = \frac{2c\tau_Y}{3\left(c^2-1\right)}, \qquad \tau_R = 0, \qquad \sigma = -\tau_Y, \tag{4.6}$$

which is an example of the solution (2.21) with $a_1 = 0$. We can imagine that the material is sitting at the yield stress waiting for the plastic flow to commence. The boundary between the flowing plastic material and the constant region is the plastic characteristic $t - t_* = X$, which represents a limiting case of the elastic-plastic boundaries discussed in §3, with $\partial\tau_1^+/\partial t = 0$ in (3.5).

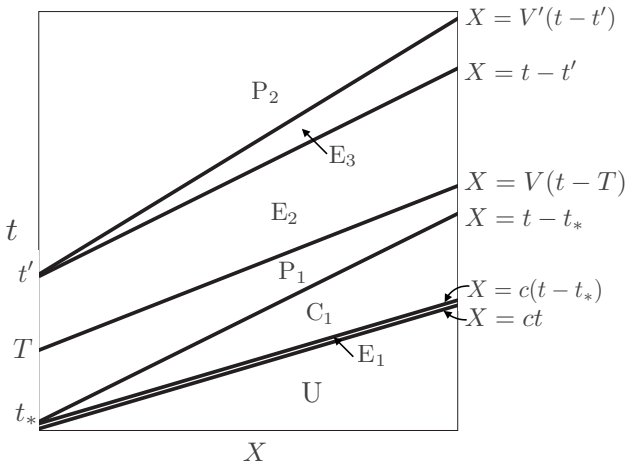

Fig. 2 A schematic of the (X, t)-plane for the loading/unloading of a linearly elastic-plastic material. The labels U, E, C and P indicate regions that are Undisturbed, Elastic, Constant and Plastic, respectively.

4.2 *Tension*

Now suppose that, after ramping up the imposed velocity for some time T, we start to decelerate the boundary, so that

$$u(0,t) = \begin{cases} t & \text{for } 0 < t < T, \\ T + \beta(T - t) & \text{for } t > T, \end{cases} \tag{4.7}$$

where $\beta > 0$. We assume that $T > t_*$ to ensure that the material is first compressed until it has passed the yield stress and then released.

The plastic solution (4.5) remains valid until the imposed acceleration at $X = 0$ changes sign at $t = T$. If we suppose that the material is still plasticised beyond the point $(0, T)$, we quickly find that causality is violated. Thus, the material instantaneously reverts to purely elastic displacements across the line $X = V(t-T)$, as indicated by the label E_2 in Figure 2, where the speed V of this elastic-plastic free boundary is to be determined. In $t > T + X/V$ we therefore solve the elastic system (2.19) subject to the boundary condition (4.7) at $X = 0$ and continuity with (4.5) across $t = T + X/V$.

We thus find the solution

$$\tau_1 = (\beta + 1)V(t - T) - t - (c - 1)t_* - \beta X, \tag{4.8a}$$

$$u = (\beta + 1)\left(T + \frac{X}{V}\right) - X - \beta t, \tag{4.8b}$$

$$\tau_R = \frac{2c\tau_Y}{3t_*}\left[T - t_* + \left(\frac{1}{V} - 1\right)X\right], \tag{4.8c}$$

$$\sigma = -\tau_Y + \frac{\tau_Y}{ct_*V}\big[(\beta + 1)V - 1\big]\big[V(t - T) - X\big], \tag{4.8d}$$

in $t > T + X/V$, along with an equation for the speed V of the elastic-plastic boundary V, namely

$$(\beta+1)V^2 + \left(c^2-1\right)V - (\beta+1)c^2 = 0. \tag{4.9}$$

There is always exactly one positive root for V. Moreover, recalling that $c > 1$, it is easily shown that this physical root lies in the range $V \in (1, c)$, in agreement with the arguments given in §3 for an elastic-plastic boundary propagating into a plastic region.

For $t > T$, yet more distinct solution regions appear. We infer from (4.8d) that the elastic material in region E_2 will eventually yield again, this time under tension, with $\sigma = +\tau_Y$. This first occurs at $X = 0$ at time

$$t = T + \frac{2ct_*}{(\beta+1)V - 1} = t'. \tag{4.10}$$

For $t > t'$ we must introduce another elastic-plastic boundary $X = V'(t - t')$, behind which there is a further plastic region P_2. We find that the new free-boundary velocity V' satisfies the equation

$$V = \frac{cV'(1+cV')}{c+V'}. \tag{4.11}$$

Given that $V \in (1, c)$, it is easily shown that $V' < 1$, in accordance with the analysis of §3, and we infer that a further boundary propagates from $(X, t) = (0, t')$ at the elastic wave speed c, with a distinct elastic region E_3 in $t' + X/c < t < t' + X/V'$, as shown in Figure 2.

We will not spell out here the solutions in regions E_3 and P_2, or the many more elastic and plastic regions that are generated as the dynamics proceeds. However, we note that, since $V > 1$, the boundary $X = V(t-T)$ between P_1 and E_2 must eventually catch up with the boundary $X = t - t_*$ between C_1 and P_1. The interaction between these two boundaries produces a complicated system of regions bounded by characteristics and free boundaries, the details of which are explored further in (**8**). In the next section, we instead move on to study another type of wave interaction by introducing a traction-free boundary at $X = 1$.

5. Reflection of compressive waves at a stress-free boundary

Motivated by experiments such as those described in (**7**), we now extend the previous analysis to the case of compression of a slab with a stress-free boundary at $X = 1$ so that

$$u(0,t) = t, \qquad \tau_1(1,t) = 0, \tag{5.1}$$

for all $t > 0$. We note that if τ_Y is either zero (no elasticity) or infinite (no plasticity), a compressive wave incident on the stress-free boundary reflects as an expansion wave and either case leads to a zigzag pattern of characteristics across which there are jumps in the first derivatives of u and τ_1. For finite values of τ_Y, the situation is more complicated as we now describe.

The regions marked E_1, C_1 and P_1 in Figure 3 are as described in §4 and illustrated in Figure 2. The reflection of the ramped elastic wave E_1 from the boundary at $X = 1$ is another ramped elastic wave E_3 which leaves behind another quiescent elastic-plastic region C_2 in which $\tau_1 \equiv 0$. Left to its own devices, the reflected wave E_3 would arrive back at $X = 0$ at time $t = 2/c$. We assume that, before this can happen, the yield stress is attained

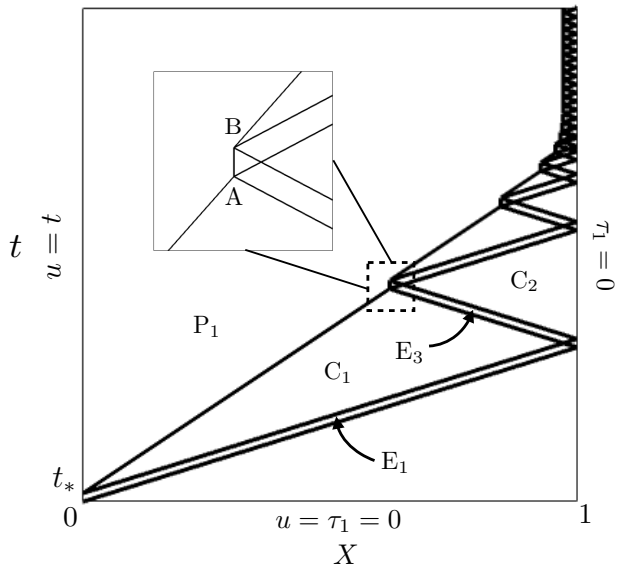

Fig. 3 Schematic of the (X, t)-plane showing reflection and reverberation of elastic characteristics at a stress-free boundary. The inset shows the intersection of the reflected elastic wave E_3 with the plastic region P_1.

at $X = 0$, resulting in the plastic wave P_1 propagating into $X > 0$ at speed 1 and interacting with E_3 in the interior of the slab. Events occur in this order provided

$$\frac{ct_*}{2} = \frac{c^2\tau_Y}{3\,(c^2-1)} < 1, \tag{5.2}$$

where t_* is the time when the material first yields at $X = 0$, defined in (4.4).

Provided the condition (5.2) is satisfied, the intersection of the reflected wave E_3 with the plastic region P_1 leads to the new elastic-plastic free boundary marked AB in the inset of Figure 3. We find that the colliding plastic and elastic waves exactly cancel each other out, resulting in the boundary AB remaining stationary at $X = (2 - ct_*)/(1 + c)$. The new elastic and plastic waves that propagate to the right from AB are precise analogues of the waves E_1 and P_1 that propagate from $X = 0$, $0 < t < t_*$. Thus the net effect of this wave interaction is to displace the leading plastic characteristic bounding the region P_1 by an amount t_* in the t-direction.

There then follows a cascade of such interactions, as sketched in Figure 3. The position of the nth displacement of the elastic plastic boundary can be shown to be at

$$X = \left(1 - \frac{ct_*}{2}\right)\left[1 - \left(\frac{c-1}{c+1}\right)^n\right], \qquad t = nt_* + \left(1 - \frac{ct_*}{2}\right)\left[1 - \left(\frac{c-1}{c+1}\right)^n\right]. \tag{5.3}$$

Hence we see that, as $n \to \infty$, the elastic-plastic free boundary approaches the exponential

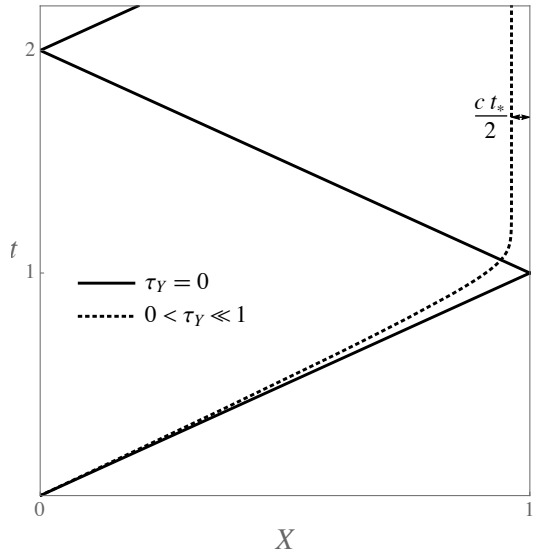

Fig. 4 Schematic of the (X,t)-plane showing the plastic wave-front in the plastic limit $\tau_Y = 0$ (solid) and with small but nonzero τ_Y (dotted).

curve

$$X \sim \left(1 - \frac{ct_*}{2}\right)\left[1 - \left(\frac{c+1}{c-1}\right)^{-c/2+(1-t)/t_*}\right]. \tag{5.4}$$

Thus, as $t \to \infty$, a fully developed state is approached in which the majority of the material is plasticised but there is a persistent elastic region near the stress-free boundary at $X = 1$. The width of this unyielded region is $ct_*/2$, which is less than 1 by (5.2), and this behaviour occurs for any value of the yield stress τ_Y which satisfies the inequality (5.2).

The dramatic "staircase" feature observed in Figure 3 is caused by interactions between elastic and plastic waves moving at different speeds. In stark contrast, in the purely plastic limit where $\tau_Y = 0$ we would simply have alternating regions of compression and expansion separated by plastic characteristics that propagate to and fro at speed 1 through the entire sample, as shown schematically by the solid curve in Figure 4. These two apparently contradictory behaviours may be reconciled by considering the behaviour when τ_Y (and therefore also t_*) is nonzero but small. In this regime, we see from (5.3) that the elastic-plastic free boundary approximately follows the plastic characteristic $X = t$ until $n = O(1/t_*)$. As the free boundary approaches $X = 1$, the collisions with the weak but nonzero elastic precursor waves accumulate, eventually eroding the plastic wave and bringing it to a halt a small but finite distance from $X = 1$, as illustrated by the dotted curve in Figure 4. Thus any nonzero yield stress, however small, completely damps the incident compressive plastic wave and prevents the reflection of a plastic release wave from the stress-free boundary.

6. Discussion and conclusions

Our modelling and analysis have illuminated some of the fascinating patterns that can emerge in the distribution of elastic and plastic regions in a uniaxially stressed slab. Even when all the waves satisfy linear wave equations, the existence of two distinct wave speeds creates the possibility of repeated interactions and reflections between elastic and plastic waves. Furthermore, the analysis of §3 reveals that the free boundary separating elastic and plastic regions in general travels at a speed equal to neither of the two intrinsic wave speeds but dependent on the applied loading. In Figure 1(a) the speed of the free boundary is less than the plastic wave speed, whereas in Figure 1(b) we have the surprising prediction that the free boundary travels faster than elastic waves; this has been termed "super-fast" wave propagation in (**5**). We remark that the characteristic diagrams in (**5**) contain the three configurations displayed in Figure 1 as well as three further configurations. These latter are non-causal in our model, and for the model considered in (**5**) they are deemed "likely to be uncommon".

The more comprehensive analysis carried out in (**8**) reveals that the configuration in Figure 1(b) can occur in the later stages of the reflection problem considered in §5 when the loading at $X = 0$ switches from compressive to tensile soon after plasticity has set in. In general, one can show that a necessary condition for the occurrence of super-fast trajectories is either that elastic waves travel in both directions or that there is a non-constant residual stress in the elastic material ahead of the free boundary (or both).

When studying the deformation of metal samples subject to very high stress, one is often interested in the limit where the dimensionless yield stress τ_Y tends to zero (**3**, **9**). In this limit, the material has zero mechanical strength, and our model apparently reduces to a single wave equation with all waves moving at the plastic wave speed. However, the problem analysed in §5 demonstrates that the regime of small but nonzero τ_Y is a singular perturbation: although the elastic precursor wave may be arbitrarily weak, repeated interactions eventually deflect the advancing plastic wave and completely suppress its reflection from the stress-free boundary.

In (**8**) it is shown that the behaviour of the plastic wavefront, illustrated by the dotted curve in Figure 4, may change markedly if either mechanical nonlinearity is introduced or a non-constant acceleration is applied at $X = 0$. Nonlinear effects cause the plastic wave-front to steepen as it advances (possibly into a shock), while a decreasing applied acceleration has the opposite effect. Depending on a delicate balance between these two influences, a plastic release wave may or may not ultimately reflect back into the sample from $X = 1$, as in the purely plastic result shown as a solid curve in Figure 4.

In this paper we have studied the simplest possible mathematical model that allows for elastic and plastic regions characterised by distinct wave-speeds. The assumptions of mechanical and geometric linearity, as well as perfect rate-independent plasticity, and our focus on analytical solutions with piecewise linear stress and velocity has led to valuable insights and predictions about the possible ways in which elastic and plastic waves and free boundaries can propagate and interact with each other. In principle one can generalise our model to include all of the effects listed above (and more). As shown in (**8**, **9**), computational solutions of the resulting nonlinear, rate-dependent equations reproduce many of the behaviours observed and explained here.

Acknowledgments

The authors would like to thank Dr D. J. Allwright, Dr C. Robinson and Dr J. Turner for many helpful discussions and suggestions. SJT was funded under the CASE studentship EP/I501592/1 with joint funding from EPSRC and AWE plc.

References

1. L. Davison, Fundementals of Shock Wave Propagation in Solids, Springer (2008).
2. P. D. Howell, G. Kozyreff and J. R. Ockendon. Applied Solid Mechanics, Cambridge (2009).
3. P. D. Howell, H. Ockendon and J. R. Ockendon. Mathematical modelling of elastoplasticity at high stress. Proc. Roy. Soc. A **468** (2012) 3842–3863.
4. L. W. Morland. The propagation of plane irrotational waves through an elastoplastic medium. Phil. Trans. Roy. Soc. **251** (1959) 341–383.
5. L. W. Morland and A. D. Cox. Existence and uniqueness of solutions to uni-axial elastic-plastic wave interactions. Phil. Trans. Roy. Soc. **264** (1969) 497–556.
6. D. C. Pack, W. M. Evans and H. J. James. The propagation of shock waves in steel and lead. Proc. Phys. Soc. **60** (1948) 1–8.
7. S. D. Rothman, J. P. Davis, J. Maw, C. M. Robinson, K. Parker and J. Palmer. Measurement of the principal isentropes of lead and lead-antimony alloy to 400 kbar by quasi-isentropic compression. Journal of Physics D: Applied Physics, **38** (2005) 733–740.
8. S. Thomson, Mathematical modelling of elastoplasticity at high stress, D. Phil. Thesis, University of Oxford (2017).
9. S. J. Thomson and P. D. Howell. A model for extreme plasticity. J. Mech. Phys. Solids, **94** (2016) 362–371.